# Status of the MUonE experiment

## G Abbiendi‡

INFN - Sezione di Bologna, Viale Carlo Berti-Pichat 6/2, 40127 Bologna, Italy E-mail: giovanni.abbiendi@bo.infn.it

Abstract. The MUonE experiment has been proposed to measure the differential cross section of  $\mu e$  elastic scattering, by colliding the 160 GeV muons of the CERN M2 beam with atomic electrons of thin target plates. From a very precise measurement of the shape one can achieve a competitive determination of the leading hadronic contribution to the muon magnetic moment, independent from the other existing ones. In preparation for the Test Run with a reduced setup the detector geometry has been optimised. Expected yields for a first physics run with limited statistics are discussed, together with prospects for the assessment of the main systematic uncertainties.

Keywords: MUonE, detector, elastic scattering, muon anomaly, vacuum polarisation, running QED coupling

### 1. Introduction

The muon magnetic moment anomaly  $a_{\mu} = (g_{\mu} - 2)/2$  is one of the most precisely measured quantities as well as one of the most precisely calculable in the Standard Model (SM), therefore it constitutes a stringent test of the theory. For the last twenty years the BNL measurement [1] has been pointing to a significant discrepancy from the theory prediction. Recently the first result from the FNAL g-2 experiment [2] has confirmed the previous measurement, and their combination brings to 4.2  $\sigma$  the deviation from the currently accepted SM prediction [3]. The theory prediction is a formidable achievement of the Standard Model, including terms up to five loops of perturbation theory for the dominant QED part, with significant contributions coming also from weak interactions and QCD. An extensive review of the state-of-the-art calculations is given in [3].

Many hypotheses have been put forward to explain this deviation as a quantum effect of new exotic particles, however it is also possible that it result from a systematic error in the calculation. The dominant uncertainty of the prediction comes from the leading order contribution from hadronic vacuum polarisation  $a_{\mu}^{\rm HVP,LO}$ , which is not calculable in perturbation theory. This is usually determined by a data-driven dispersive approach, using the low-energy measurements of hadronic production in  $e^+e^-$  annihilation [4, 5]. In contrast, a recent ab initio calculation of  $a_{\mu}^{\rm HVP,LO}$  based on Lattice QCD [6] reduces the discrepancy with the measurement, and is in tension with the data-driven estimates.

In the next years the FNAL experiment is expected to increase the precision by about a factor of 4, while another forthcoming experiment at J-PARC [7] should reach a similar precision. Therefore it is of paramount importance to improve the theory calculation and clarify the comparison of the available estimates. A novel approach has been proposed in [8], to determine the leading hadronic contribution  $a_{\mu}^{\text{HVP},\text{LO}}$  from a measurement of the effective electromagnetic coupling in the space-like region, where the vacuum polarisation is a smooth function. Its master equation is:

$$a_{\mu}^{\text{HVP, LO}} = \frac{\alpha}{\pi} \int_0^1 dx \, (1 - x) \, \Delta \alpha_{\text{had}}[t(x)] \,, \tag{1}$$

where  $\Delta \alpha_{\rm had}(t)$  is the hadronic contribution to the running of the QED coupling, evaluated at the space-like (negative) squared four-momentum transfer:

$$t(x) = -\frac{x^2 m_\mu^2}{1 - x} < 0. (2)$$

The running QED coupling is expressed as:

$$\alpha(t) = \frac{\alpha(0)}{1 - \Delta\alpha(t)},\tag{3}$$

where  $\alpha(0) = \alpha$  is the fine-structure constant, and

$$\Delta \alpha(t) = \Delta \alpha_{\text{lep}}(t) + \Delta \alpha_{\text{had}}(t). \tag{4}$$

The hadronic contribution  $\Delta \alpha_{\text{had}}(t)$  can be extracted by subtracting from  $\Delta \alpha(t)$  the purely leptonic part  $\Delta \alpha_{\text{lep}}(t)$ , which can be calculated to very high precision in QED.

To date there exist very few direct measurements of the running of  $\alpha$  in the spacelike region, the most precise one was obtained by the OPAL experiment [9], from smallangle Bhabha scattering at LEP, and reached the sensitivity for the observation of the hadronic contribution.

Based on the method of [8], the MUonE experiment [10] has been proposed, to measure the hadronic running of  $\alpha(t)$  from  $\mu e$  elastic scattering at low energy. This method could reach a competitive precision below 0.5% on the  $a_{\mu}^{\text{HVP,LO}}$ , provided the systematic errors are kept under control. The MUonE project has been submitted to the CERN SPS Committee with the Letter-of-Intent [11] in 2019. A Test Run has been approved with a partial apparatus as a validation of the detector design and of the overall concept.

In this paper the current status of the project is summarised, and some recent developments are described. Section 2 describes the proposed MUonE setup with a recent geometry optimisation. Section 3 reviews the analysis technique in some detail, and section 4 discusses the achievable yields in the forthcoming Test Run, highlighting the sensitivity to the main systematic effects which have to be dealt with. Section 5 lists the main theoretical advancements which constitute the other important face of the challenge. Finally the conclusions are given in section 6.

## 2. MUonE experimental apparatus

The idea of the MUonE experiment has been put forward in [10]. The hadronic running of the QED coupling needed in the master equation (1) can be determined by a very precise measurement of the shape of the differential cross section of  $\mu e$  elastic scattering, using the CERN M2 muon beam ( $E_{\mu} \sim 150\text{-}160 \text{ GeV}$ ) off atomic electrons of a light target. This process has several attractive features:

- simple kinematics;
- pure t-channel;
- useful centre-of-mass energy to probe the dominant region for the muon q-2;
- easy selection based on the correlation of the electron and muon scattering angles.

The proposed detector has been described in [11]. The scattering angles of muons and electrons are measured by tracking stations as the one represented in Figure 1. An elastic scattering event produced in the thin target plate in front of the station, with thickness of 1.5 cm, is identified by measuring the two outgoing tracks in three pairs of planes made of silicon microstrips with orthogonal strips, over a length of one meter. The tracking precision is crucial, so in addition to a good intrinsic resolution it is necessary to limit the multiple Coulomb scattering. For this purpose the target has to be made of a low-Z material as beryllium or carbon and has to be thin. To reach the necessary interaction rate while preserving these conditions a modular layout is proposed, forming

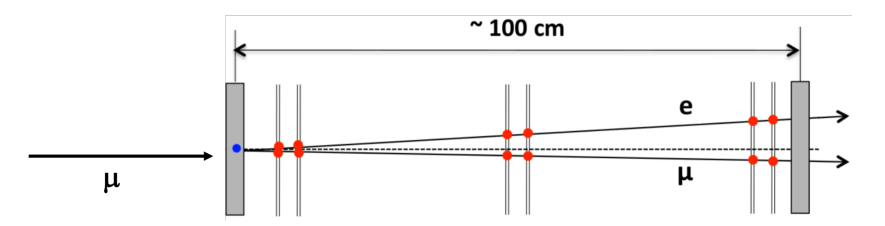


Figure 1. Scheme of one tracking station.

an array of identical stations crossed by the muon beam, as shown in Figure 2. The

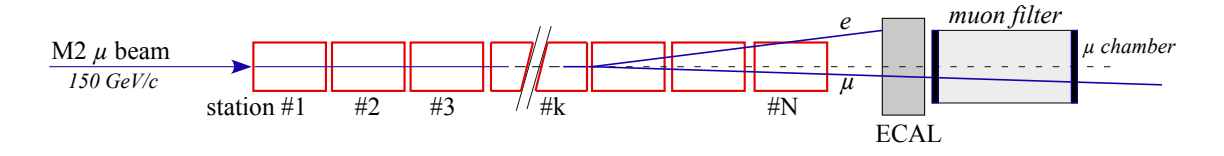


Figure 2. Layout of the MUonE experimental apparatus (not to scale).

full apparatus consists of 40 such stations, followed by an electromagnetic calorimeter (ECAL) and a muon detector at the end, to help the identification and the selection. Beam muons are almost unaffected by the upstream detector material, except for a small energy loss, so every station behaves as an independent detector. The events occurring at a given station have the incoming muon direction measured by the preceding station. This configuration could reach the target statistical sensitivity in three years of run at the M2 beam, collecting an integrated luminosity of  $1.5 \times 10^7$  nb<sup>-1</sup> [11].

The basic tracking unit has been chosen to be the 2S module developed for the upgrade of the CMS outer tracker [12]. It consists of two close-by planes of silicon microstrips, separated by 1.8 mm, with strips along the same direction in the two sensors and reading the same coordinate. A pair of matching hits in the two sensors gives a so-called stub, or track element, providing track triggering capability at 40 MHz, with inherent suppression of background from single-layer hits or large-angle tracks. It has a large active area of about  $10 \times 10 \text{ cm}^2$ , allowing to completely cover the relevant MUonE angular acceptance with a single module, thus assuring the best uniformity. With respect to the LHC operation the main difference for MUonE will be the asynchronous nature of the signals from the  $\mu e$  scattering events. This will be managed by a specific configuration of the front-ends, and will be studied in detail during the Test Run.

### 2.1. Detector optimisation

The hit intrinsic resolution of the tracking detector is particularly important. This is clearly demonstrated by Monte Carlo simulations based on GEANT4 [13, 14]. Figure 3 shows the distributions obtained for the scattering angles of the muon and the electron, reconstructed from the simulated hit patterns, corresponding to two different tracking

setups. In both cases the reconstructed events include both the signal (elastic scattering events) and background events from  $e^+e^-$  pair production, which can mimic elastic events when one electron goes undetected. The top plot corresponds to the performance obtained in a beam test with the UA9 detector [15], which achieved a position resolution of  $7\mu$ m on individual hits. The bottom plot corresponds to the performance obtained in another beam test [16], which featured a worse resolution of  $\sim 35\text{-}40\mu\text{m}$ . A good intrinsic resolution is crucial to allow for an effective separation of the signal from the background by cutting on the muon scattering angle at  $\theta_{\mu} \geq 0.1 - 0.2$  mrad.

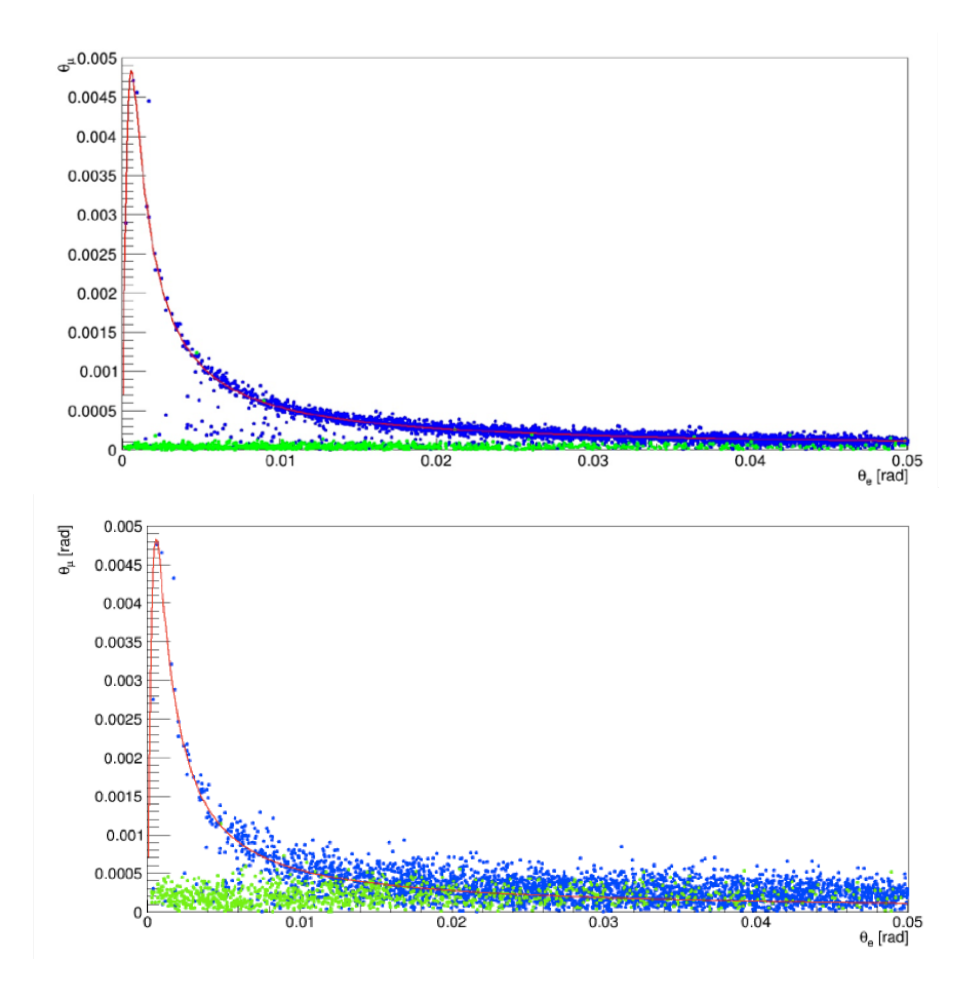


Figure 3. Simulated angular distributions of two-track events, expected for 150 GeV beam muons in: (Top) the UA9 detector of [15]; (Bottom) the detector used in the beam test of [16]. The blue points represent  $\mu e$  events, the green ones background events with production of an  $e^+e^-$  pair in the material. The red curve represents the ideal elastic scattering. Plots from [17].

The CMS 2S module has a strip pitch of  $90\mu m$  and operates with digital readout. Hence hits recorded from single-strip clusters will have a resolution of about  $90\mu m/\sqrt{12} \simeq 26\mu m$  on a single detection plane, which does not seem optimal for MUonE. Possible improvements were suggested by an independent study taking the MUonE detector as a case study [18]. Following these hints a detailed study was carried

out by a full simulation describing both the geometry and the digitisation of the 2S module.

The ionisation charge produced by the passage of a charged particle through the silicon layer is collected on the strips, giving a digital signal when it exceeds a configurable threshold, which is typically set around 6 times the RMS electronic noise level. A well-known method to improve the resolution of silicon strip detectors consists in tilting the planes around an axis parallel to the strips. This was recently applied to the CHROMIE telescope [19]. This simple geometry change increases the probability of charge sharing between adjacent strips and can produce a significant number of clusters with two strips above threshold, which results in a better estimate of the crossing point of the track. The optimal working point is expected to correspond to an average cluster width of 1.5 strips, which happens when an equal amount of one- and two-strip clusters is found. An additional improvement can be obtained by an effective staggering of the two sensor layers constituting the 2S module. In fact a micro-tilt of 25 mrad is equivalent to an half-strip staggering of the two sensor layers. The two effects, charge sharing between adjacent strips of the same layer and staggering of the two sensor layers constituting the 2S module, can sum up to obtain a larger improvement. The search for the optimal working point was carried out by comparing several different simulations obtained for different values of the signal threshold and the tilt angle. The best result was obtained for a tilt angle of 233 mrad and signal threshold at 6 times the RMS noise level, with a resolution of  $8.0\mu m$ . For comparison, the resolution for the non-tilted geometry, with the sensors orthogonal to the beam direction, was found to be about  $22\mu m$ . The study also tested the robustness of the result under mechanical imperfections in the 2S module assembly, in particular a possible misalignment of the two sensor layers along the measurement coordinate, orthogonal to the strip direction, which would be equivalent to an unwanted staggering of the two layers. Considering the expected mechanical precision this would lead to a slightly worsened resolution of  $11\mu m$ . In conclusion the study demonstrated that the simplest idea of an half-strip staggering of the two sensor layers alone, to be realised in hardware, would not provide a stable working point, while the effect of a substantial tilt of the detector geometry is robust.

As a consequence, the mechanical design of a MUonE tracking station has been updated as shown in Figure 4. The structure length is still one meter. The target plate is followed by three equally-spaced XY supermodules, each one made of two closeby 2S modules with orthogonal strips. The first and last supermodules, measuring X and Y transverse coordinates, have tilted modules by 233 mrad, as determined by the study. The middle supermodule is rotated by 45° around the beam axis, to resolve reconstruction ambiguities, and its modules are not tilted. There are stringent requirements on the mechanical stability of the tracking stations, which has to be better than  $10\mu$ m, in particular on the longitudinal size. Therefore the support structure is made of Invar (Fe-Ni alloy), which has a very low coefficient of thermal expansion, is easy to machine and relatively cheap. A cooling system is also designed, in addition to an enclosure to stabilise the room temperature within  $1^{o}$ - $2^{o}$ .

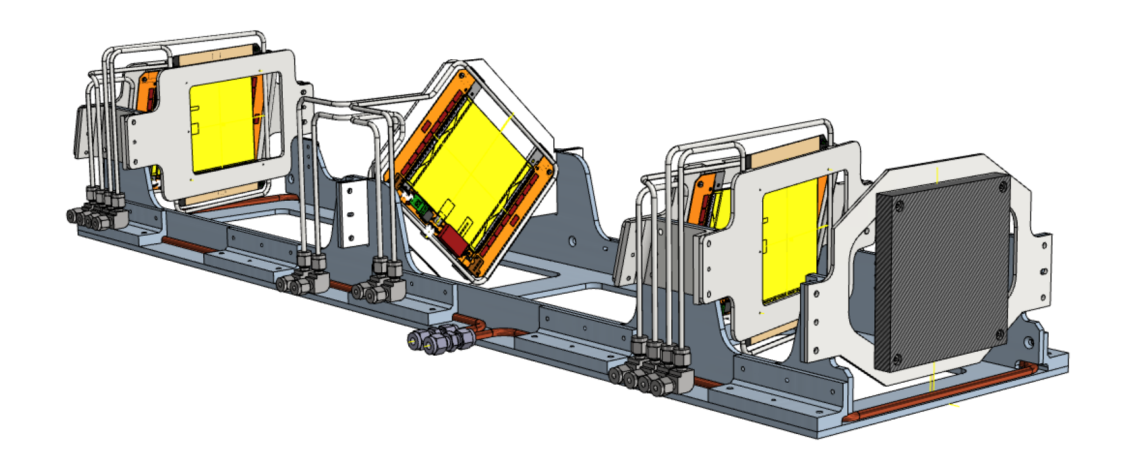


Figure 4. CAD drawing of a MUonE tracking station.

## 3. MUonE analysis technique

The hadronic contribution to the running of  $\alpha$  is most easily displayed by considering the ratio  $R_{\text{had}}$  of a cross section including the full running of  $\alpha$  and the same cross section with no hadronic running. At Leading Order (LO) the cross section has simply the squared coupling factorised, so this approximation holds:

$$R_{\rm had}^{LO}(t) = \frac{d\sigma^{LO}(\Delta\alpha_{\rm had}(t) \neq 0)}{d\sigma^{LO}(\Delta\alpha_{\rm had}(t) = 0)} \simeq 1 + 2\Delta\alpha_{\rm had}(t).$$
 (5)

For a muon beam energy of 160 GeV, the centre-of-mass energy is  $\sqrt{s} = 0.418$  GeV and the maximum momentum transfer is  $t_{max} = -0.175 \text{ GeV}^2$ . The hadronic contribution  $\Delta \alpha_{\rm had}(t)$  has a tiny variation across the probed kinematical range  $0 < |t| < |t_{max}|$ changing from a vanishingly small value at low |t| to about  $10^{-3}$  at the peak of the integrand in (1), which occurs at  $t = -0.108 \text{ GeV}^2$  (x = 0.914). A competitive determination of  $a_{\mu}^{\rm HVP,\,LO}$  requires a precision of  $\mathcal{O}(10^{-2})$  in the measurement of the hadronic running, which translates into an unprecedented precision of  $\mathcal{O}(10^{-5})$ in the shape of the differential cross section. Reaching this accuracy requires a huge statistics of data, in the order of few times 10<sup>12</sup> events. Therefore even preliminary simulation studies would present a computational challenge. A smart trick applicable to the simulation studies consists in using the very same MC sample to determine the  $R_{\rm had}$  ratios, by reweighting events to include or exclude the hadronic component of  $\alpha(t)$ . The distribution simulating real data (the *pseudodata*) is determined with the hadronic running switched on, and is fluctuated for the expected statistical uncertainties corresponding to the desired luminosity. The distribution representing the theory prediction is determined with the hadronic running switched off and neglecting the statistical uncertainties, assuming that it will be the case in the end. In this way in the ratio of these two distributions almost all the correlated uncertainties due to limited statistics will cancel out and the signal from the hadronic running will be visible.

Obviously this trick works only with the MC simulation, while with real data one will have to match the generated MC statistics to the number of real data.

At Next-to-Leading Order (NLO) the ratios  $R_{\rm had}$  can be defined for observables like the scattering angles by using a more complex reweighting technique, considering the structure of the matrix element in events with the emission of a real photon. No attempt is done to estimate the momentum transfer t event by event. Actually radiative events strongly modify the LO kinematics and their correct description is necessary. The analysis described in [11] used a NLO Monte Carlo generator implementing an exact calculation including masses  $(m_{\mu}, m_e)$  and electroweak corrections in a fully differential code [20]. The hadronic contribution  $\Delta \alpha_{\rm had}(t)$  is included in the generator by the Jegerlehner numerical parameterisation [21, 22], which is obtained from the dispersive integral of low-energy measurements of hadronic production in  $e^+e^-$  annihilation and perturbative QCD. This parameterisation gives  $a_{\mu}^{\rm HVP, LO} = 688.6 \times 10^{-10}$  when it is inserted into the master integral (1). Other existing parameterisations can be used as well.

Beam spread and detector resolution effects are included in a fast simulation. The muon beam is given a spread of 3.75% around its nominal value of 150 GeV with a Gaussian distribution. The intrinsic angular resolution for the measured tracks is assumed to be  $\sigma_{\theta} = 0.02$  mrad. The multiple Coulomb scattering is parameterised by a Gaussian with the usual approximation for the width [23].

The extraction of the hadronic contribution is carried out by a template fit method, in which the templates for the observed distribution are calculated by reweighting the MC events to correspond to an appropriate functional form of  $\Delta \alpha_{\rm had}(t)$ . Several analytical forms have been tested. A third order polynomial could in principle describe the MUonE data but is unphysical, and it would make the integrand in (1) divergent for  $x \to 1$ . A Padé approximant with three free parameters, like:

$$\Delta \alpha_{had}(t) = at \frac{1+bt}{1+ct} \tag{6}$$

would be well behaved. However the best found option is a physically inspired parameterisation, corresponding to the one-loop QED calculation of vacuum polarisation induced by a lepton pair in the space-like region:

$$\Delta \alpha_{had}(t) = k \left\{ -\frac{5}{9} - \frac{4M}{3t} + \left( \frac{4M^2}{3t^2} + \frac{M}{3t} - \frac{1}{6} \right) \frac{2}{\sqrt{1 - \frac{4M}{t}}} \log \left| \frac{1 - \sqrt{1 - \frac{4M}{t}}}{1 + \sqrt{1 - \frac{4M}{t}}} \right| \right\}, \tag{7}$$

where the M parameter replaces the squared lepton mass  $m^2$  and k the factor  $\alpha/\pi$ . The same form is also valid for the contribution of  $t\bar{t}$  pairs (with  $M=m_{top}^2$  and  $k=\frac{\alpha}{\pi}Q^2N_c$ , with Q=2/3 the top electric charge and  $N_c=3$  the number of colours). Since the hadronic contribution to the running  $\alpha$  is not calculable in perturbation theory, the parameters k and M do not have a precise physics interpretation. At large |t| the dependency is logarithmic, proportional to  $\log(|t|/M)$  as expected. In the limit of very small t it reduces to a linear trend:

$$\Delta \alpha_{had}(t) \simeq -\frac{1}{15} \frac{k}{M} t, \tag{8}$$

which corresponds to the dominant behaviour in the MUonE kinematical region. Correcting terms, corresponding to quadratic and higher orders in t are incorporated in the form of (7).

The Lepton-Like parameterisation (7) has been preliminarily tested against the Jegerlehner numerical parameterisation. The level of agreement is excellent, considering that (7) has only two free parameters. In comparison the Padé form (6) cannot fit equally well the Jegerlehner parameterisation. In addition, having three instead of two free parameters, it leads to larger uncertainties in the resulting integral (1).

The template fit is carried out by defining a grid of points (k, M) in the parameter space covering a region of  $\pm 5\sigma$  around the expected values, with  $\sigma$  being the expected uncertainty. Actually, due to the dominant low-t dependence, the k and M parameters are highly correlated and it is convenient to use K = k/M as fit parameter, substituting k = KM in (7). The step size is taken to be  $0.5\sigma$ . This defines  $21 \times 21 = 441$  templates for the relevant distributions. Figure 5 shows a few representative templates in the chosen window for the angular distribution of the scattered muon, together with the central values expected for the MUonE nominal luminosity. Every template in the grid

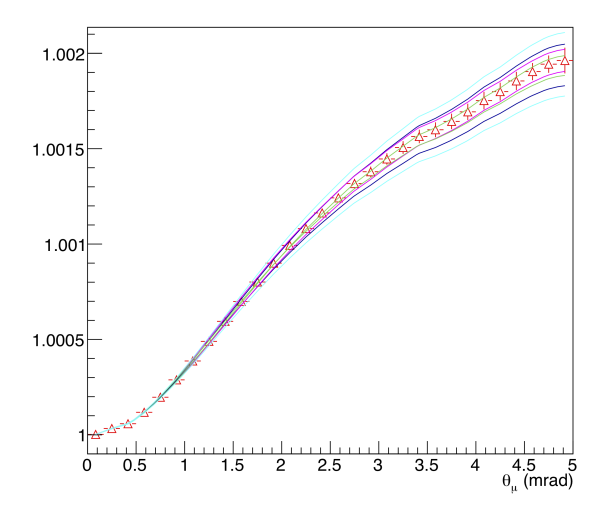


**Figure 5.** Central prediction for  $R_{\rm had}(\theta_{\mu})$ . The error bars correspond to the expected statistical uncertainties for the nominal MUonE luminosity of  $1.5 \times 10^7$  nb<sup>-1</sup>. The curves show a few representative MC templates.

is compared to the pseudodata calculating:

$$\chi^{2}(K,M) = \sum_{i} \frac{R_{i}^{data} - R_{i}^{templ}(K,M)}{\sigma_{i}^{data}},$$
(9)

where the sum runs over all the bins, and the minimum  $\chi^2$  is found by parabolic interpolation across the grid points. The error is determined for  $\Delta \chi^2 = 1$ .

The fit can be done on the distribution of the muon or the electron scattering angle, as well as on their two-dimensional distribution, which gives the most accurate result. Actually there is almost no need to identify the outgoing muon and electron, provided

the event is a signal one. In this case the two track angles are labelled as  $\theta_L$  and  $\theta_R$ , meaning Left or Right with respect to an arbitrary axis.

The geometric acceptance of the MUonE stations covers the relevant region of scattering angle  $\theta \leq 32$  mrad, which in LO corresponds to outgoing electrons with energy greater than 1 GeV. It is important to remind that only the shape of the angular distributions is relevant, the absolute normalisation is neglected, as it will suffer from a relatively large systematic uncertainty related to the luminosity determination. The fitted parameterisation (7) is then inserted into the master integral (1), and the value of  $a_{\mu}^{\text{HVP,LO}}$  is determined by integrating over the full phase space. Figure 6 shows the  $R_{\text{had}}$  distributions obtained for the muon and electron angle, for an example pseudoexperiment, with the fit result superimposed. The statistical accuracy of the

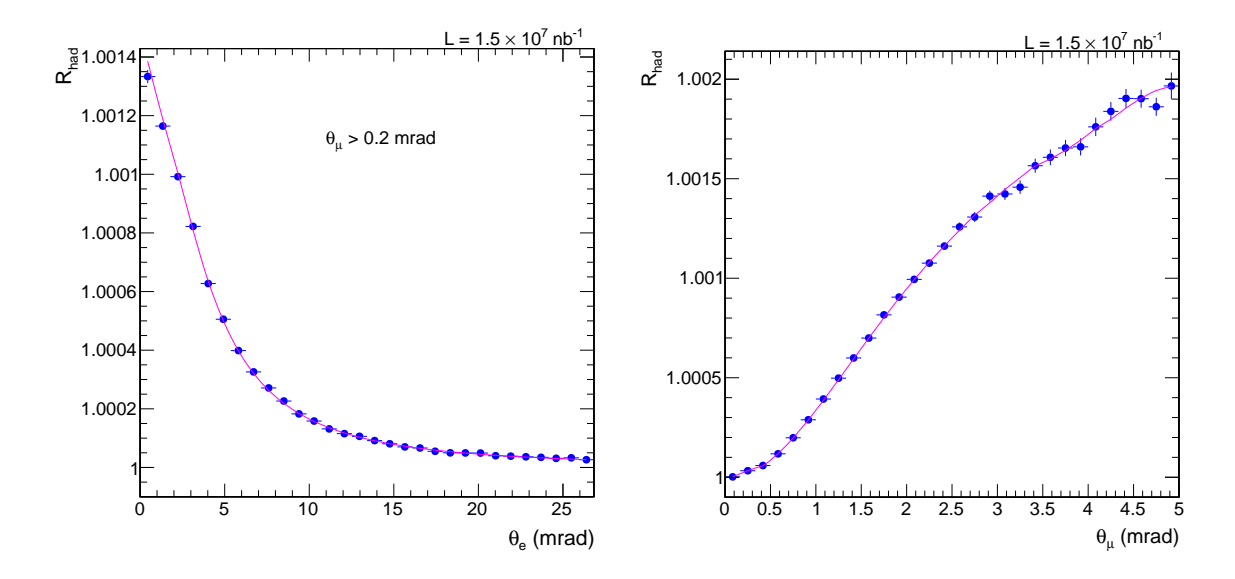


Figure 6. Example pseudodata showing the ratios  $R_{\text{had}}$  for (Left) the electron angular distribution, after a cut at  $\theta_{\mu} > 0.2$  mrad, and (Right) the muon angular distribution. The error bars show the statistical uncertainties corresponding to the nominal MUonE luminosity. The template fit is superimposed.

fit has been tested by repeating many pseudoexperiments, each one with statistics equivalent to the MUonE nominal luminosity. From 1,000 pseudoexperiments we get  $a_{\mu}^{\rm HVP,LO} = 688.8 \pm 2.4 \times 10^{-10}$  which is in very good agreement with the expected value of the Jegerlehner parameterisation used in the generator (688.6 × 10<sup>-10</sup>). With respect to the result obtained in [11] we have improved the fit technique, basically removing the systematic uncertainty related to the fit model which we had mentioned there. Further studies will be carried out using other input models.

## 4. Test Run

A first important milestone is a three-week Test Run at the CERN M2 beam line, with full intensity muon beam. The selected location is upstream of the COMPASS detector,

after its Beam Momentum Spectrometer (BMS) [24]. The MUonE setup will consist of two tracking stations followed by the ECAL, with an additional station (without target) upstream to track the incoming muons [11]. Initially the Test Run was allocated in fall 2021. However there were some delays in the procurement of the module components and a shift in the CMS preproduction timeline, so the final schedule has to be redefined.

This forthcoming Test Run shall confirm the detector design and engineering and constitute a proof of concept for the many challenges to be faced. Among these, the procedures for the alignment (hardware and software), the readout chain and the trigger strategy to identify and reconstruct  $\mu e$  events.

The physics potential of the Test Run setup has been estimated by considering the standard SPS efficiency with full beam intensity, and allowing for the necessary time for detector commissioning [25]. The two stations could yield  $\sim 1 \text{ pb}^{-1}/\text{day}$ , and reasonably we could integrate up to  $\sim 5 \text{ pb}^{-1}$  of good data during a first physics run, with a safety margin for possible data-taking inefficiencies. This integrated luminosity would correspond to  $\sim 10^9 \mu e$  scattering events with electron energy greater than 1 GeV.

The expected event yields are shown in Figure 7 for the electron and muon angular distributions. The muon distribution has a dip at very small angles, which results from

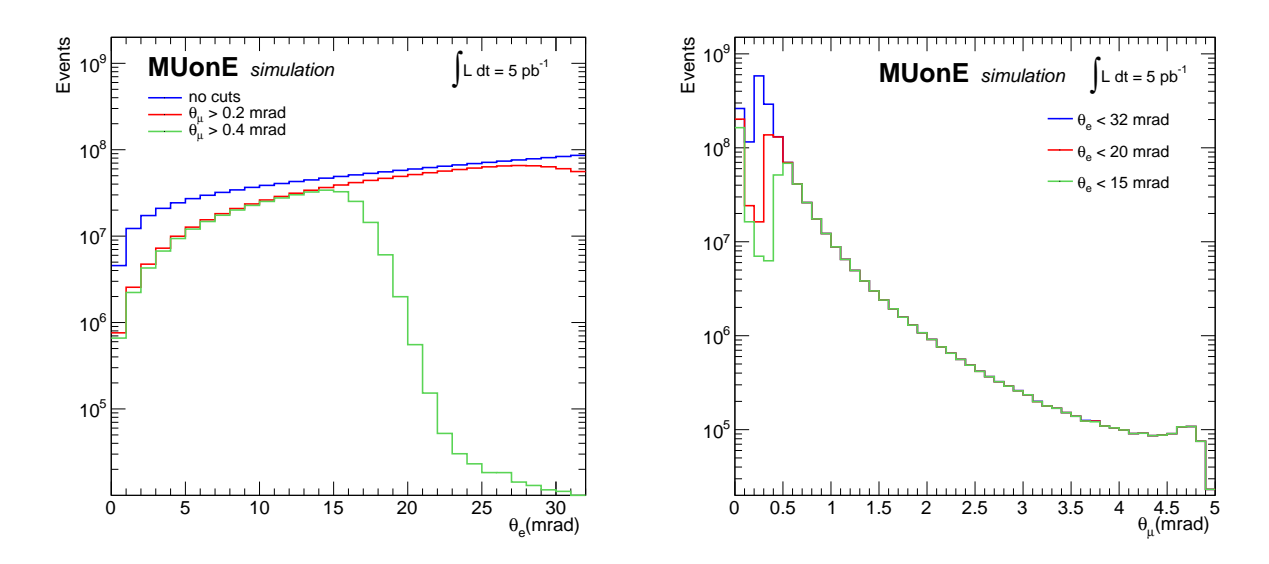


**Figure 7.** Event yields expected in the Test Run, for: (*Left*) the electron and (*Right*) the outgoing muon, after the application of simple angular cuts.

the  $\theta_e < 32$  mrad geometric acceptance for the outgoing electron. Tighter cuts on the electron angle produce a wider dip on the muon distribution. Muons entering the dip region result from events with one real photon emitted, which smear the perfect correlation expected for elastic events. A minimal cut  $\theta_{\mu} > 0.2$  mrad, aimed to reject radiative events, strongly affects the shape of the electron angular distribution, as shown in Figure 7 (*Left*). The removed events are characterised by low-energy electrons which would contaminate the signal region at small  $\theta_e$ . By applying a tighter cut on the muon angle, as  $\theta_{\mu} > 0.4$  mrad, the electron distribution is cut for angles greater than 15-20 mrad. The visible edge is smeared by detector resolution and radiative events.

The statistics achievable at the Test Run would give enough sensitivity to measure the leptonic running of  $\alpha$  and potentially could provide initial sensitivity to the hadronic running. With respect to the nominal luminosity, the fit method has been adapted to a simpler case. The parameter M in (7) is fixed to its expected value  $M=0.0525~{\rm GeV^2}$  and only K=k/M is fitted, to determine a linear deviation on the shape. Fig. 8 shows the expectation for the muon  $R_{\rm had}$  distribution with a few template distributions superimposed. From 1,000 pseudoexperiments the central value of the fit is found to be  $K=0.136\pm0.026$ . This represents the slope of the observable hadronic running at the purely statistical level.

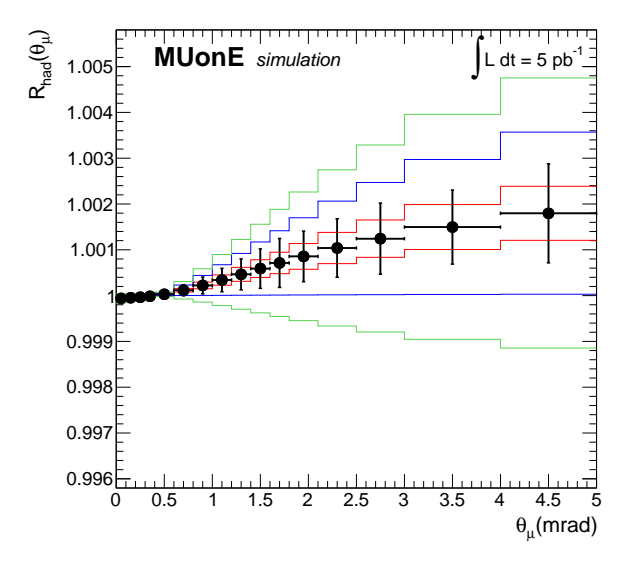


Figure 8. Ratio  $R_{\rm had}$  of the expected muon angular distribution and the prediction obtained with only leptonic running in  $\alpha(t)$ . The error bars correspond to the statistical uncertainties for an integrated luminosity of 5 pb<sup>-1</sup> assumed for the Test Run. The histograms show the templates for few values of the slope K. Plot from [25].

It is important to assess the expected systematic errors, which will have to be fully understood in the Test Run conditions to estimate their impact in the full-scale experiment. The most important systematic effects will be measured from the data itself, in the so-called *normalisation region*, where the hadronic running is negligible. This corresponds to events where the muon is scattered at small angle keeping most of its initial energy, while the emitted electron goes at relatively large angles with energy of few GeVs. The recorded statistics in this region will be very large allowing for very precise measurements of the detector performance.

The intrinsic resolution is one of the most important figures to be determined. It will be routinely monitored while carrying out the track-based detector alignment. However a more precise measurement is required by the physics analysis. A sharp

control over this parameter is possible by applying a cut on the muon angle at  $\theta_{\mu} > 0.4$  mrad and observing the shape of the resulting edge in the electron angle distribution. Figure 9 (*Left*) shows the expected distortion which would be visible for a  $\pm 10\%$  systematic error on the intrinsic angular resolution. Reversing the roles, Figure 9 (*Right*) shows the effect which would be seen in the muon angle distribution after applying a cut on the electron angle at  $\theta_e < 20$  mrad.

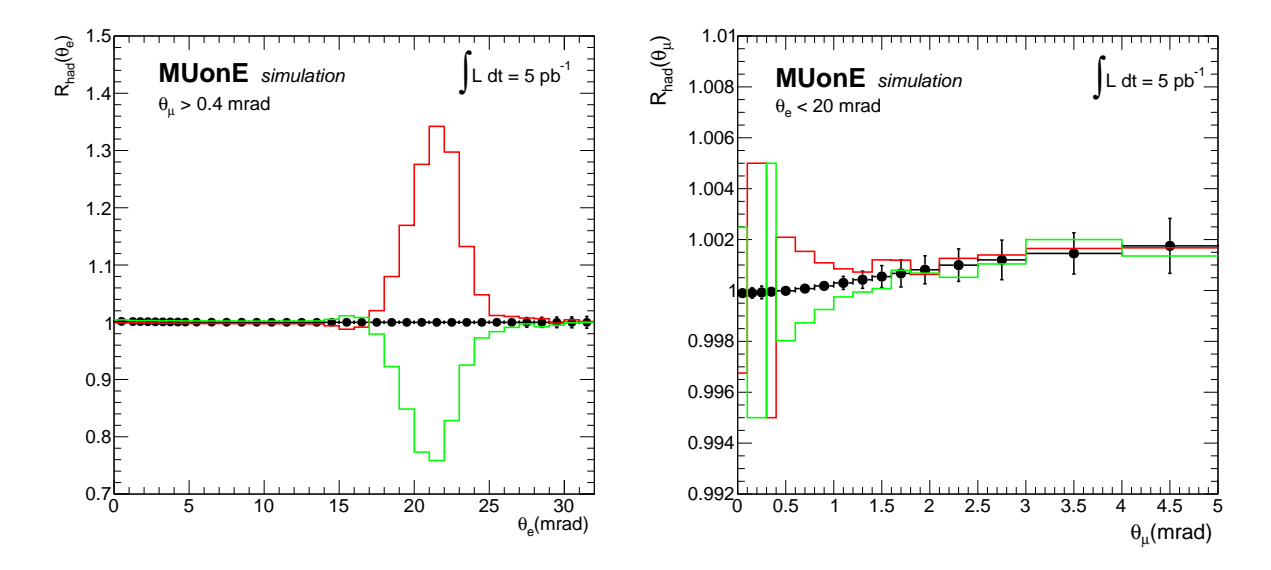


Figure 9. Effect of a systematic error of +10% (red histograms) or -10% (green histograms) in the intrinsic angular resolution of the detector (expected  $\sigma_{\theta} = 0.02$  mrad), as visible in the  $R_{\rm had}$  ratios: (*Left*) the electron distribution after a cut at  $\theta_{\mu} > 0.4$  mrad; (*Right*) the muon distribution, after a cut at  $\theta_{e} < 20$  mrad. The solid points represent the expected central values with error bars showing the statistical uncertainties for the Test Run.

The final detector resolution will depend also on the material effects, in particular the multiple Coulomb scattering (MCS), mostly affecting the low energy electrons. MCS of 12 GeV and 20 GeV electrons on thin carbon targets has been studied in a dedicated beam test in 2017 [15]. The core of the measured angular distributions was found to agree within  $\pm 1\%$  with the predictions from the GEANT4 simulation. The effect of a flat  $\pm 1\%$  error on the MCS core width, respectively on the muon and the electron angular distributions is shown in Figure 10.

The observable patterns produced by systematic errors on the detector resolution are so evident that a first natural step will consist in a calibration of these effects by fitting the data in control regions. After this first calibration the residual systematic uncertainties will be included as nuisance parameters in a likelihood fit and will be determined simultaneously with the signal parameters. We have tested the capability of doing such a simultaneous fit by using the combine tool [26, 27], a software package used for statistical analysis within CMS, based on RooStats/RooFit [28]. The two systematic effects related to the detector resolution described above have been included,

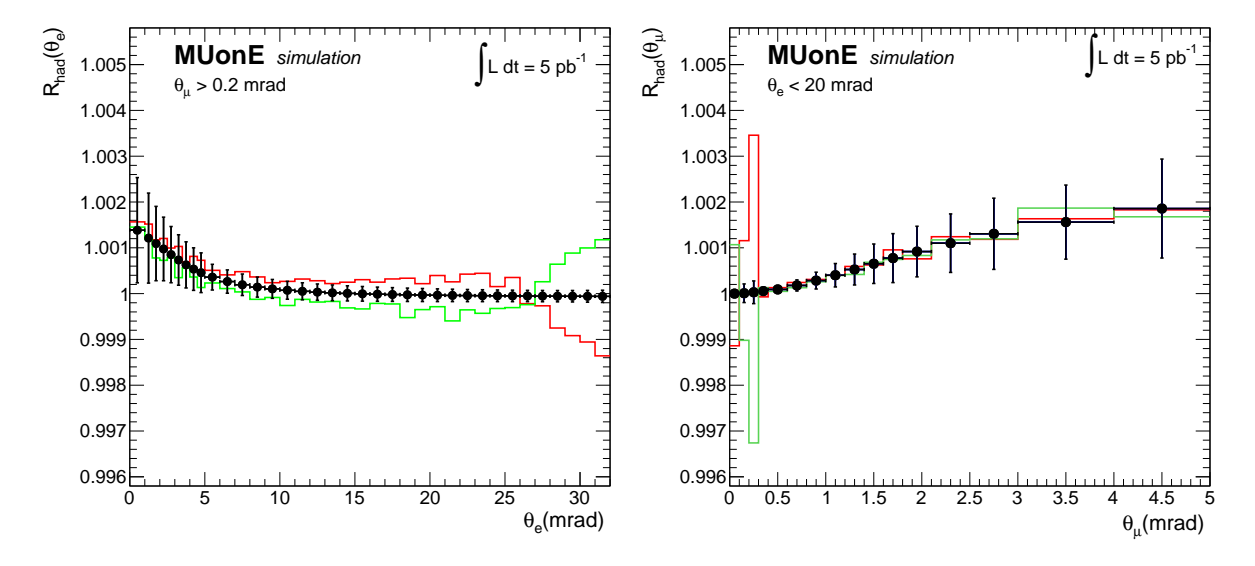


Figure 10. Effect of a systematic error of +1% (red histograms) or -1% (green histograms) on the assumed width of the core of the MCS distribution, as seen in the  $R_{\text{had}}$  ratios: (*Left*) the electron distribution after a cut at  $\theta_{\mu} > 0.2$  mrad, and (*Right*) the muon distribution (from [25]). The solid points represent the expected central values with error bars showing the statistical uncertainties for the Test Run.

together with a normalisation nuisance representing the luminosity uncertainty. Angular distributions corresponding to the effects of  $\pm 1\sigma$  for each systematic source taken alone have been provided as input to the tool, for every value of the physics parameter K. Then, for each of these K values the nuisance parameters are fitted from the pseudodata. The best fit for the signal parameter K is then found by parabolic interpolation over the grid points. Since the nuisance parameters are weakly correlated with the physics parameter K, their final values could also be easily approximated by interpolation. Otherwise, if needed, one could do a second step, by fixing the K value to the best fit for it and producing  $\pm 1\sigma$  templates around it to do this last minimisation. The fit has proved to be reliable within the covered range of uncertainties ( $\pm 10\%$  for the intrinsic angular resolution and  $\pm 1\%$  for the core width of MCS). Input pseudodata with systematic errors within this range have been successfully fitted, with almost no degradation for the fitted signal parameter K. As said, this works so well as the signal and the nuisances mostly act on different kinematical regions.

Another crucial systematic effect is related to the knowledge of the average beam energy scale. This is known from the accelerator at a level of about 1%. The BMS spectrometer can measure individual incoming muons with 0.8% resolution, and given the high muon beam intensity it can provide an excellent monitor of time variations of the average scale. However it cannot assess the systematic uncertainty of the average energy scale, which has to be controlled by a physical process. The kinematics of the elastic  $\mu e$  scattering has been identified as the useful method [11], in particular the

average angle of the two outgoing tracks, which does not need  $\mu$ -e identification. For illustration purpose Figure 11 shows the effect on the muon angular distribution of a systematic error of  $\pm (0.1\text{-}1.0)$  GeV on the assumed average beam energy. The expected distortion is compared to the statistical uncertainty corresponding to one hour running time in one station. It is clear that the energy calibration by the kinematical method would already outperform the precision of the scale obtained from the accelerator. The beam energy scale will be calibrated on each tracking station independently, aiming at an ultimate precision for the final detector better than 3 MeV in less than one week of run.

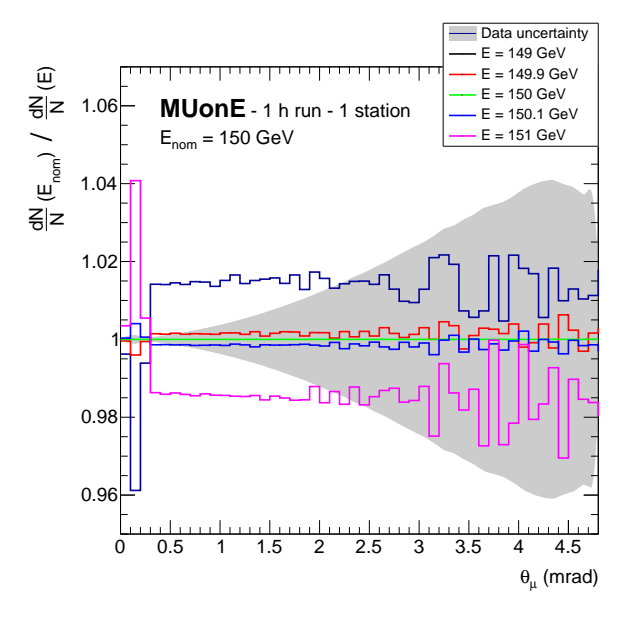


Figure 11. Effect of a shift of  $\pm (0.1\text{-}1.0)$  GeV in the average beam energy with respect to the nominal value  $E_{\text{nom}} = 150$  GeV. The histograms show the expected distortions on the muon angular distribution, obtained from MC samples with variable energy. The grey band represents the statistical uncertainty corresponding to the expected data collected in one hour running time by one station. Plot from [25].

## 5. Theoretical progress

An intense theoretical activity has been going on in the last years, to obtain the very precise calculations needed for the MUonE measurement. A comprehensive review [34] describes the full NLO calculation, including both QED and electroweak corrections, also made available in a fully exclusive MC event generator [20], the calculation of NNLO hadronic corrections [29, 30], and the evaluation of the two-loop integrals relevant for the NNLO QED corrections [31, 32, 33].

Very recently, the analytic evaluation of the two-loop corrections to the process  $e^+e^- \rightarrow \mu^+\mu^-$  has been completed [35], treating the electron (muon) as massless (massive) particle.

Another very recent paper [36] presented simple exact analytic expressions to compute the hadronic vacuum polarisation contribution to the muon g-2 in the space-like region up to next-to-leading order. These results can be employed by MUonE to extend the determination of  $a_{\mu}^{\rm HVP}$  from leading to next-to-leading order.

Moreover, the exact NNLO photonic corrections on the leptonic legs, including all mass terms, have been implemented in two independent and fully exclusive MC codes [37, 38]. Their results have been compared and are in very good agreement. In addition, the complete NNLO corrections including a lepton pair have been calculated and implemented in the MESMER MC code [39]. Resummation of leading terms in higher orders (by parton shower and YFS exponentiation) matched to (N)NLO will be necessary and is being carried out. Finally, the possible contaminations of the MUonE measurement of  $a_{\mu}^{\rm HVP,LO}$  from new physics effects have been studied and found to be below the detection sensitivity [40, 41].

## 6. Conclusions

The MUonE experiment could help understanding the puzzle of muon g-2, by providing a third way to determine the leading order hadronic contribution  $a_{\mu}^{\rm HVP,LO}$ , independent of the traditional method using the dispersive integral of time-like measurements and of the lattice QCD calculations. The availability of precise calculations will be important in the next years, with the improving precision expected from the Fermilab g-2 experiment and the J-PARC project. The expected statistical precision of 0.35% for the MUonE determination of  $a_{\mu}^{\rm HVP,LO}$  constitutes a competitive benchmark, which demands a strict control on all the systematic uncertainties to be reached.

In this paper we have presented the status of the project, describing in particular an optimisation of the detector geometry which can improve the hit spatial resolution by more than a factor of 2, with respect to the setup described in our Letter of Intent. The analysis technique has also grown up recently and is reviewed here in some details. We have presented simulation results concerning some of the most important systematic effects, as they could be seen and directly measured at the forthcoming Test Run. The tasks are challenging but no showstopper has been found.

The experimental activities in preparation of the Test Run are progressing. Initial tests with few modules have started in fall 2021. The foreseen setup will be integrated and tested as soon as the hardware components become available, compatibly with the SPS schedule.

A full experimental proposal will be prepared after the Test Run completion, assuming it to be successful. The full detector construction could then take place, with the prospect of a substantial running time during the LHC Run3, before the start of the Long Shutdown scheduled in 2026-2028.

## References

- [1] G. W. Bennett *et al.* [Muon g-2 Collaboration], "Final Report of the Muon E821 Anomalous Magnetic Moment Measurement at BNL", *Phys. Rev. D* **73** (2006) 072003, [arXiv:hep-ex/0602035].
- [2] B. Abi et al. [Muon g-2 Collaboration], "Measurement of the Positive Muon Anomalous Magnetic Moment to 0.46 ppm", Phys. Rev. Lett. 126 (2021) 141801, [arXiv:2104.03281].
- [3] T. Aoyama *et al.*, "The anomalous magnetic moment of the muon in the Standard Model", *Phys. Rept.* **887** (2020) 1, [arXiv:2006.04822].
- [4] M. Davier, A. Hoecker, B. Malaescu and Z. Zhang, "A new evaluation of the hadronic vacuum polarisation contributions to the muon anomalous magnetic moment and to  $\alpha(m_Z^2)$ ", Eur. Phys. J. C 80 (2020) 241 [erratum: Eur. Phys. J. C 80 (2020) 410], [arXiv:1908.00921].
- [5] A. Keshavarzi, D. Nomura and T. Teubner, "g-2 of charged leptons,  $\alpha(M_Z^2)$ , and the hyperfine splitting of muonium", *Phys. Rev. D* **101** (2020) 014029, [arXiv:1911.00367].
- [6] S. Borsanyi, et al., "Leading hadronic contribution to the muon magnetic moment from lattice QCD", Nature 593 (2021) 51, [arXiv:2002.12347].
- [7] M. Abe *et al.*, "A New Approach for Measuring the Muon Anomalous Magnetic Moment and Electric Dipole Moment", *PTEP* **2019** (2019) 053C02, [arXiv:1901.03047].
- [8] C. M. Carloni Calame, M. Passera, L. Trentadue and G. Venanzoni, "A new approach to evaluate the leading hadronic corrections to the muon g-2", Phys. Lett. B 746 (2015) 325, [arXiv:1504.02228].
- [9] G. Abbiendi et al. [OPAL Collaboration], "Measurement of the running of the QED coupling in small-angle Bhabha scattering at LEP", Eur. Phys. J. C 45 (2006) 1, [arXiv:hep-ex/0505072].
- [10] G. Abbiendi *et al.*, "Measuring the leading hadronic contribution to the muon g-2 via  $\mu e$  scattering", Eur. Phys. J. C 77 (2017) 139, [arXiv:1609.08987].
- [11] G. Abbiendi *et al.* [MUonE Collaboration], "Letter of Intent: the MUonE project", CERN-SPSC-2019-026 / SPSC-I-252.
- [12] CMS Collaboration, "The Phase-2 Upgrade of the CMS Tracker", CERN-LHCC-2017-009 / CMS-TDR-014.
- [13] S. Agostinelli *et al.* [GEANT4 Collaboration], "GEANT4 a simulation toolkit", *Nucl. Instrum. Meth. A* **506** (2003) 250.
- [14] J. Allison et al. "Recent developments in Geant4", Nucl. Instrum. Meth. A 835 (2016) 186.
- [15] G. Abbiendi *et al.*, "Results on multiple Coulomb scattering from 12 and 20 GeV electrons on carbon targets", *JINST* **15** (2020) P01017, [arXiv:1905.11677].
- [16] G. Abbiendi *et al.*, "A study of muon-electron elastic scattering in a test beam", *JINST* **16** (2021) P06005, [arXiv:2102.11111].
- [17] A. Principe, "Feasibility study of the MUonE experiment: measuring the leading hadronic contribution to the muon g-2 via space-like data", Bologna (2019) master thesis, https://amslaurea.unibo.it/18533.
- [18] T. Dorigo, "Geometry optimization of a muon-electron scattering detector", *Physics Open* 4 (2020) 100022, [arXiv:2002.09973].
- [19] P. Asenov [CMS], "Commissioning and simulation of CHROMIE, a high-rate test beam telescope", JINST 15 (2020) C02003, [arXiv:2002.02313].
- [20] M. Alacevich, C. M. Carloni Calame, M. Chiesa, G. Montagna, O. Nicrosini and F. Piccinini, "Muon-electron scattering at NLO", *JHEP* **02** (2019) 155, [arXiv:1811.06743].
- [21] S. Eidelman and F. Jegerlehner, "Hadronic contributions to g-2 of the leptons and to the effective fine structure constant  $\alpha(M_Z^2)$ ", Z. Phys. C67 (1995) 585, [arXiv:hep-ph/9502298].
- [22] F. Jegerlehner, "The Running fine structure constant  $\alpha(E)$  via the Adler function", Nucl. Phys. B Proc. Suppl. 181-182 (2008) 135, [arXiv:0807.4206].
- [23] G.R. Lynch and O.I. Dahl, "Approximations to multiple Coulomb scattering", Nucl. Instrum. Meth. B 58 (1991) 6.

- [24] P. Abbon et al. [COMPASS Collaboration], "The COMPASS experiment at CERN", Nucl. Instrum. Meth. A 577 (2007) 455, [arXiv:hep-ex/0703049]
- [25] G. Abbiendi [MUonE Collaboration], "Status of the MUonE experiment", PoS ICHEP2020 (2021) 223, [arXiv:2012.07016].
- [26] ATLAS and CMS Collaborations, LHC Higgs Combination Group, "Procedure for the LHC Higgs boson search combination in Summer 2011", CMS NOTE 2011/005, ATL-PHYS-PUB 2011-11 (2011).
- [27] combine: https://cms-analysis.github.io/HiggsAnalysis-CombinedLimit/
- [28] L. Moneta, K. Belasco, K. S. Cranmer, S. Kreiss, A. Lazzaro, D. Piparo, G. Schott, W. Verkerke and M. Wolf, "The RooStats Project", PoS ACAT2010 (2010) 057, [arXiv:1009.1003].
- [29] M. Fael, "Hadronic corrections to  $\mu$ -e scattering at NNLO with space-like data", *JHEP* **02** (2019) 027, [arXiv:1808.08233].
- [30] M. Fael and M. Passera, "Muon-Electron Scattering at Next-To-Next-To-Leading Order: The Hadronic Corrections", *Phys. Rev. Lett.* **122** (2019) 192001, [arXiv:1901.03106].
- [31] P. Mastrolia, M. Passera, A. Primo and U. Schubert, "Master integrals for the NNLO virtual corrections to  $\mu e$  scattering in QED: the planar graphs", *JHEP* **11** (2017) 198, [arXiv:1709.07435].
- [32] S. Di Vita, S. Laporta, P. Mastrolia, A. Primo and U. Schubert, "Master integrals for the NNLO virtual corrections to μe scattering in QED: the non-planar graphs", JHEP 09 (2018) 016, [arXiv:1806.08241].
- [33] S. Di Vita, T. Gehrmann, S. Laporta, P. Mastrolia, A. Primo and U. Schubert, "Master integrals for the NNLO virtual corrections to  $q\bar{q} \to t\bar{t}$  scattering in QCD: the non-planar graphs", *JHEP* **06** (2019) 117, [arXiv:1904.10964].
- [34] P. Banerjee et al., "Theory for muon-electron scattering @ 10 ppm: A report of the MUonE theory initiative", Eur. Phys. J. C 80 (2020) 591, [arXiv:2004.13663].
- [35] R. Bonciani, A. Broggio, S. Di Vita, A. Ferroglia, M. K. Mandal, P. Mastrolia, L. Mattiazzi, A. Primo, J. Ronca and U. Schubert, "Two-Loop Four-Fermion Scattering Amplitude in QED", Phys. Rev. Lett. 128 (2022) 022002, [arXiv:2106.13179].
- [36] E. Balzani, S. Laporta and M. Passera, "Hadronic vacuum polarization contributions to the muon g-2 in the space-like region", [arXiv:2112.05704].
- [37] C. M. Carloni Calame, M. Chiesa, S. M. Hasan, G. Montagna, O. Nicrosini and F. Piccinini, "Towards muon-electron scattering at NNLO", *JHEP* 11 (2020) 028, [arXiv:2007.01586].
- [38] P. Banerjee, T. Engel, A. Signer and Y. Ulrich, "QED at NNLO with McMule", SciPost Phys. 9 (2020) 027, [arXiv:2007.01654].
- [39] E. Budassi, C. M. Carloni Calame, M. Chiesa, C. L. Del Pio, S. M. Hasan, G. Montagna, O. Nicrosini and F. Piccinini, "NNLO virtual and real leptonic corrections to muon-electron scattering", JHEP 11 (2021) 098, [arXiv:2109.14606].
- [40] A. Masiero, P. Paradisi and M. Passera, "New physics at the MUonE experiment at CERN", Phys. Rev. D 102 (2020) 075013, [arXiv:2002.05418].
- [41] P. S. B. Dev, W. Rodejohann, X. J. Xu and Y. Zhang, "MUonE sensitivity to new physics explanations of the muon anomalous magnetic moment", JHEP 05 (2020) 053, [arXiv:2002.04822].